Binding and Oxidation of Alkyl 4-Nitrophenyl Ethers by Rabbit Cytochrome P450 1A2: Evidence for Two Binding Sites†

Grover P. Miller and F. Peter Guengerich*

Department of Biochemistry and Center in Molecular Toxicology, Vanderbilt University School of Medicine, Nashville, Tennessee 37232-0146

Received February 26, 2001; Revised Manuscript Received April 17, 2001

ABSTRACT: Although most cytochrome P450 (P450) reactions demonstrate saturation kinetics that fit to the standard Michaelis−Menten equation, there are important exceptions where sigmoidal or nonhyperbolic behavior is observed and have been fit instead to kinetic models involving two binding sites. To assess these models, we demonstrate the consistency of a two binding site model to interpret both steady-state kinetics and binding events. Rates of 4-nitrophenol and formaldehyde production from the *O*-demethylation of 1-methoxy-4-nitrobenzene by P450 1A2 isolated from rabbit liver produced biphasic plots, when plotted against substrate concentration. Experiments confirmed the absence of the further oxidation of the products. Recombinant rabbit P450 1A2 yielded the same maximal velocity and more marked biphasicity. Overall, these steady-state data fit well to kinetic models involving two binding sites. Steady-state studies of substrates with bulkier *O*-ethyl or *O*-isopropoxy groups indicated decreased affinity for the second site. Based on binding studies, the affinity of P450 1A2 for these substrates increased 200-fold with the larger alkyl groups. To analyze the single binding site model, competition studies were conducted with 1,4-phenyldiisocyanide and the alkyl 4-nitrophenyl ethers. Although the observed dissociation constants and the competing titrant demonstrated a linear dependence, the affinity for the competing titrant depended on the presence of the other titrant, which violates the single binding site model. Alternatively, we applied a two binding site model to these data to obtain dissociation constants for the binary and ternary complexes. The agreement between the dissociation constants for the heterogeneous complexes supports the appropriateness of the two binding site model. This novel finding for P450 1A2 may be more common than originally perceived for P450s.

P450[1] enzymes encompass a large class of heme-thiolate monooxygenase enzymes found throughout nature and occur in multiple forms within a single species. These enzymes catalyze the oxidation of the majority of drugs, pollutants, pesticides, and carcinogens as well as endogenous compounds such as steroids, alkaloids, amino acids, and eicosanoids. The importance of these reactions in cellular processes has made the understanding of P450 mechanisms of action a focus of intense research (*2*−*4*). The knowledge of catalytic mechanisms is an integral part of the elucidation of enzyme specificity, an important topic in areas as diverse as drug design, bioremediation, and cancer risk estimation.

A majority of P450 reactions demonstrate hyperbolic saturation kinetics, of which the interpretation of data typically involves the standard Michaelis−Menten scheme. Nevertheless, there are several examples of P450 reaction kinetics that are not described by this simple single-site mechanism. In these cases, the oxidation of substrate by P450 results in sigmoidal or nonhyperbolic behavior. Typically, these data are fit to the Hill equation, which is an empirical description of cooperativity. Although the Hill coefficient derived from this equation has no physical meaning, it does provide a qualitative description of the nature of the cooperativity between enzyme and substrates, as well as inhibitors. Sigmoidal kinetics reflect positive cooperativity in which the affinity for substrate increases at higher substrate concentrations. Negative cooperativity induces nonhyperbolic curvature because higher concentrations of substrate inhibit the ability of the enzyme to reach the maximal velocity.

Atypical reaction kinetics are a hallmark of P450 3A4, whose catalytic properties for substrates and inhibitors are rather complex. Several substrates involve sigmoidal kinetics, including aflatoxin B_1 (*5*), steroids (*6*, *7*), carbamazepine (*8*, *9*), amitriptyline (*9*), and diazepam (*10*). The extent of the observed cooperativity often depends on the presence of competing substrates or inhibitors. Attempts to reconcile these ligand−ligand interactions include proposals of mechanisms involving one to three nonequivalent binding sites (*5*, *9*−*12*). For example, Shou et al. (*10*, *13*) proposed a kinetic model for P450 3A4 involving two cooperative substrate binding sites, which successfully rationalized

† This work was supported in part by U.S. Public Health Service (USPHS) Grants R35 CA44353 and P30 ES00267. G.P.M. was supported in part by USPHS Postdoctoral Fellowship F32 GM19808.

* To whom correspondence should be addressed at the Department of Biochemistry and Center in Molecular Toxicology, Vanderbilt University School of Medicine, 638 Medical Research Building I, 23rd and Pierce Ave., Nashville, TN 37232-0146. Tel.: 615-322-2261; Fax: 615-322-3141; E-mail: guengerich@toxicology.mc.vanderbilt.edu.

[1] Abbreviations: P450, cytochrome P450 [also termed "heme-thiolate P450" by the Enzyme Commission (EC 1.14.14.1) (*1*)]; NPR, NADPH−P450 reductase; DLPC, L-α-dilauroyl-*sn*-glycero-3-phosphocholine; CHAPS, 3-[(3-choloamidopropyl)dimethylammonio]-1-propanesulfonic acid.

10.1021/bi010402z CCC: $20.00
Published on Web 05/15/2001

Scheme 1: Oxidation of 1-Methoxy-4-nitrobenzene by Rabbit Liver P450 1A2

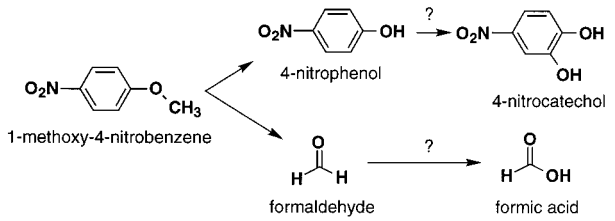

sigmoidal reaction kinetics of substrates in the presence and absence of inhibitors. In a related study, this kinetic model was applied to the sigmoidal metabolism of naphthalene by P450s 2B6, 2C8, 2C9, and 3A5 and the nonhyperbolic metabolism of naphthalene by P450 3A4 and naproxen by P450 2C9 (*9*). The ability of kinetic models to assess the feasibility of reaction mechanisms is a step toward deepening our understanding of P450 catalysis.

A weakness of these proposals is the absence of data demonstrating the presence of multiple binding sites. Recently Hosea et al. (*11*) provided indirect evidence for the presence of more than one binding site for P450 3A4. The strategy relied on the interactions between a peptide (YPNP-NH_2) and P450 3A4 to inhibit binding and catalysis for a series of substrates, i.e., testosterone, midazolam, and α-naphthoflavone. The binding of the peptide was competitive with respect to the substrates, such that the observed dissociation constant increased as a function of peptide concentration, but the spectral amplitude of the titration and the extent of cooperativity did not. Based on these binding studies, the mechanism of inhibition suggested that there exist two binding sites for the peptide, a higher affinity one overlapping with testosterone and midazolam and a lower affinity site overlapping with α-naphthoflavone (*11*).

There are several reasons that can account for the difficulties involved in P450 binding studies. A hallmark of P450 research has been the utility of the absorbance spectrum of the heme group. Changes in the coordination of iron ligands yield observable spectral changes, which often correlate with the binding of molecules in the active site. Nevertheless, only some P450s possess useful spectral properties for binding studies. Another complication arises from the typical hydrophobicity of the substrate, which either prevents the saturation of the binding site due to poor solubility or results in an affinity greater than the minimal concentration of P450 required to determine accurately the dissociation constant.

In light of these considerations, we utilized a model system involving the *O*-demethylation of 1-methoxy-4-nitrobenzene by rabbit P450 1A2. This substrate exhibits higher solubility than typical P450 substrates and has attractive spectral properties for continuous monitoring of the reaction. Oxidation of this substrate yields 4-nitrophenol and formaldehyde, although the potential exists for further oxidation to 4-nitrocatechol and formic acid (Scheme 1). To confirm the homogeneity of the rabbit liver P450 1A2 preparation, the cDNA was subcloned and expressed in *Escherichia coli*. The catalytic properties of the purified recombinant rabbit P450 1A2 were then compared to the liver enzyme. This study was extended to include substrates with bulkier *O*-ethyl or *O*-isopropoxy groups to address the steric limitations of the P450 1A2 binding site. For binding studies, the heme properties of rabbit liver P450 1A2 offer both typical P450 Type I and Type II spectra (*14*) during a binding event. These binding modes for the substrate enabled the design of competitive binding studies between the alkyl 4-nitrophenyl ethers and 1,4-phenyldiisocyanide to assess the validity of the single binding site model. Taken together, we demonstrate the consistency of a two binding site model to interpret both steady-state kinetics and binding events.

EXPERIMENTAL PROCEDURES

Materials. All reagents were purchased from Fisher Scientific (Pittsburgh, PA) or Sigma Chemical (St. Louis, MO). The substrates 1-methoxy-4-nitrobenzene (*p*-nitroanisole) and 1-ethoxy-4-nitrobenzene (*p*-nitrophenetole) and the product 4-nitrophenol were obtained from Aldrich Chemical Co. (Milwaukee, WI). Since 4-nitrophenyl compounds often contain many impurities, all substrates were recrystallized 2−3 times from C_2H_5OH/H_2O to yield slightly yellowish white solids. Propagation of plasmid DNA was carried out using *E. coli* DH5α cells. Restriction and DNA modifying enzymes were purchased from New England Biolabs (Beverly, MA). Primers for PCR reactions were obtained from the Vanderbilt University DNA Core Facility. All P450 assays were conducted using the buffer 100 mM potassium phosphate, pH 7.4, containing 50 μM DLPC at 30 °C. Because binding titrations of 1-methoxy-4-nitrobenzene using stocks (up to 2 mM) made in CH_3CN or reaction buffer yielded identical results, we were confident of the high solubility of the substrate in reaction buffer.

Preparation of 1-Isopropoxy-4-nitrobenzene. Of the substrates used in this study, 1-isopropoxy-4-nitrobenzene is not commercially available. Synthesis of this compound was accomplished by heating of 4-nitrophenol, 2-bromopropane, and K_2CO_3 in acetone at reflux overnight (*15*). The resulting reaction mixture was filtered and then evaporated to dryness in vacuo. The solid was resuspended in CH_2Cl_2 and washed twice with 1 N NaOH to remove excess 4-nitrophenol. The CH_2Cl_2 layer was recovered, dried over anhydrous Na_2SO_4, and concentrated in vacuo using a rotary evaporator to yield a yellowish solid. The product was recrystallized twice from C_2H_5OH/H_2O, 1:1 (v/v) (mp 31−32 °C) (*16*). Mass spectra yielded the expected molecular ion (MH^+ at *m*/*z* 181.2) [done using an HP 5890A gas chromatograph (Hewlett-Packard Co., Wilmington, DE) coupled to a Finnigan MAT INCOS 50 mass spectrometry (Finnigan MAT, San Jose, CA)]. The ^1H NMR spectrum was consistent with the structure: δ 1.29 (d, 6H, $CH(CH_3)_2$), 4.57 (m, 1H, $CH(CH_3)_2$), and 6.86 (d, 2H, phenyl) and 8.14 (d, 2H, phenyl), in $CDCl_3$ using a Bruker AM 400 spectrometer operating at 400.13 MHz and 27 °C (Bruker, Billerica, MA).

Recombinant Rabbit P450 1A2 Expression Plasmid. Although the full-length rabbit P450 1A2 cDNA has never been reported and is not available, a large fragment (1.2 kbp) was obtained from Norio Kagawa (Vanderbilt University). To construct the full-length gene, a two-step strategy was employed. First, the polymerase chain reaction was performed using rabbit P450 1A1 (from Norio Kagawa) as a template and mutagenic primers (Table 1). The 5′ portions of rabbit P450s 1A1 and 1A2 share high identity in this region. Next, the PCR product and the P450 1A2 cDNA fragment were combined for a second reaction using the

Table 1: Primers Used in the Construction of the Recombinant Rabbit P450 1A2 Expression Plasmid

primers	sequence[a]
For(−)9/del(7−39)[b] (overlap step)	GGAGGTCATATGGCGCTGCTGCTGGTC-AGCGCGGTCTTCTGCCTGGTG
For67[c]	CTGGTGTTCTGGGCGGTGCGCGCGAGC-CGCCCGAAGGTACCGAAA
Rev344	GCTGTACAGGTCAGGCG
For331	CTGTACAGCAGCAGCTTCATCACCGAA-GGCCAGAGCATGAACTTCAGCCCAGA
Rev1533H6[d]	CCGCGCATCTCTAGATTATCA-GTGATGATGGTGATGGTGCTGGTVG-GAGAAGCGTGGGCG

[a] All sequences are written 5′ to 3′. [b] Underlined sequence denotes an *Nde*I site. [c] Underlined sequence denotes a *Kpn*I site. [d] Underlined sequence denotes the 6-histidine tag.

primers for the 5′ and 3′ ends of the cDNA (Table 1). There are two reactions at this step, which differ in the 3′ primer used. One primer includes six extra codons encoding six histidines (a C-terminal His-tag) whereas the other does not. The overlap extension product was subjected to restriction digestion by *Nde*I and *Hin*dIII and then ligated into the expression vector pCW. The polymerase chain reactions were performed using *Pfu* polymerase essentially as described by the manufacturer (Stratagene, La Jolla, CA), using a Perkin-Elmer 9600 Thermocycler.

Expression and Purification of Rabbit P450 1A2. Rabbit liver P450 1A2 was prepared as previously described (*17, 18*). The preparation of the recombinant P450 1A2 required a modified procedure. The expression of recombinant rabbit P450 1A2 in *E. coli* DH5α was accomplished as described, and *E. coli* membranes containing recombinant P450 1A2 were prepared (*18*). Membranes were solubilized for 3 h at 4 °C at a final concentration of 2 mg of protein mL^{-1} in 100 mM potassium phosphate buffer (pH 7.4) containing 20% glycerol (v/v), 1.0 mM EDTA, 10 mM β-mercaptoethanol, and 1.0% CHAPS (w/v). The solubilized material was then loaded onto a 3 mL column of Ni^{2+}-nitrilotriacetate resin (Qiagen, Valencia, CA) that had been preequilibrated with 100 mM potassium phosphate buffer (pH 7.4) containing 20% glycerol (v/v), 0.5 M NaCl, 5 mM imidazole, and 0.5% CHAPS (v/v). Contaminating proteins were removed by extensive washing with the equilibration buffer containing 20 mM imidazole. P450 1A2 was eluted from the column with 100 mM potassium phosphate buffer (pH 7.4) containing 20% glycerol (v/v), 300 mM imidazole, 0.5 M NaCl, and 0.5% CHAPS (w/v). Fractions containing P450 were pooled and dialyzed at 4 °C for 24 h against a 200-fold volume of 100 mM potassium phosphate buffer (pH 7.4) containing 20% glycerol (v/v), 1.0 mM EDTA, and 0.10 mM dithiothreitol, followed by two more changes of the same buffer without dithiothreitol. [With human, rat, and rabbit P450 1A2 enzymes, high ionic strength (100 mM phosphate) should be maintained to prevent precipitation (*18*).] Sodium dodecyl sulfate−polyacrylamide gel electrophoresis was used to assess final protein purity, and P450 concentrations were determined by Fe^{2+}·CO versus Fe^{2+} difference spectroscopy (*19*).

Steady-State Kinetic Parameters. For consistency, all of the steady-state studies were conducted using the identical conditions discussed below. Since P450 catalysis requires an accessory protein, NPR, an initial experiment involved varying the NPR to P450 ratio until turnover was optimized with 0.2 μM rabbit P450 1A2, and the NPR concentration varied from 0.1 to 0.8 μM such that the P450:NPR ratio ranged from 1:0.5 to 1:4. The steady-state rate was determined by measuring the rate of 4-nitrophenol formed from oxidation of 1-methoxy-4-nitrobenzene (100 μM). The turnover rate at a ratio of 1:0.5 P450:NPR increased 20% as the ratio was increased to 1:2 P450:NPR (results not shown). Adding more NPR did not change the observed rate; thus, all steady-state studies reflect the 1:2 P450:NPR ratio, which is often used with P450 systems (*20*).

Two approaches were employed to assess steady-state turnover by rabbit P450 1A2. First, catalysis was monitored continuously using the spectroscopic signals for substrate 4-nitrophenyl ether and product 4-nitrophenol. Second, formaldehyde production required a discontinuous assay involving quantitation of formaldehyde at selected time points. The assay conditions for this study were based on prior work optimizing human P450 1A2-catalyzed *O*-deethylation of 7-ethoxycoumarin (*21*). The reaction mixture consisted of 0.25 μM P450 1A2, 0.50 μM NPR [recombinant rat enzyme expressed in *E. coli* (*22, 23*)], DLPC (50 μM), 100 mM potassium phosphate buffer (pH 7.4), 1% CH_3CN (used to dissolve the substrate for the stock solution), an NADPH-generating system [0.2 mM $NADP^+$, 10 mM glucose 6-phosphate, and 1.0 IU of glucose-6-phosphate dehydrogenase mL^{-1} (*20*)], and varying concentrations of substrate (0.2−1500 μM depending on the respective substrate) at 30 °C.

For continuous assays, a 1.0 mL reaction was initiated upon addition of NADPH, and its progression was monitored at the maximal absorbance either for substrate 1-methoxy-4-nitrobenzene (314 nm) or for product 4-nitrophenol (400 nm) for 10 min using a Cary14/OLIS spectrophotometer (On-Line Instrument Systems, Bogart, GA). The respective extinction coefficients were determined empirically under the reaction conditions (1-methoxy-4-nitrobenzene, $\epsilon_{314} = 10.4\ mM^{-1}\ cm^{-1}$; 4-nitrophenol, $\epsilon_{400} = 12\ mM^{-1}\ cm^{-1}$). For the other substrates, 1-ethoxy-4-nitrobenzene and 1-isopropoxy-4-nitrobenzene, only 4-nitrophenol production was measured as a function of time.

In contrast, the determination of the rate of formaldehyde production from 1-methoxy-4-nitrobenzene oxidation requires a discontinuous approach whereby formaldehyde must be quantitated as a function of time to derive a progress curve. Because the Nash reaction (*24*) and a procedure using the purpald reagent (4-amino-3-hydrazino-5-mercapto-1,2,4-triazole) (*25*) proved to be both inconsistent and insensitive for formaldehyde quantitation, a modified version of a published HPLC procedure was used to determine the initial rates of formaldehyde production as a function of 1-methoxy-4-nitrobenzene concentration (*26, 27*). The approach entailed the derivatization of formaldehyde with 2,4-dinitrophenylhydrazine. Quantitation of the product was accomplished by HPLC against a set of standards. Reaction progression was monitored using a 6 mL reaction and taking five 1.0 mL aliquots over a 10 min period. The reaction sample was quenched with 0.15 mL of 25% $HClO_4$ containing 50 μM valeraldehyde as an internal standard. The mixture was incubated on ice for 10 min and centrifuged at $10^4 g$ for 15 min. An aliquot of the supernatant (1.0 mL) was transferred

to a 5.0 mL reaction vial containing 1.0 mL of hexanes and 0.1 mL of freshly prepared 2,4-dinitrophenylhydrazine in 6 N HCl. After rotation-mixing the reaction for 1 h at room temperature, a 0.65 mL aliquot of the hexane layer was transferred to a glass test tube containing 0.20 mL of CH_3CN. The hexane layer was extracted by vortex-mixing twice for 5 s. A 0.15 mL aliquot of the CH_3CN layer was transferred to an HPLC vial containing 0.15 mL of H_2O.

To quantitate the amount of formaldehyde produced, aliquots (50 μL) of the recovered supernatants were injected onto an ODS Partisil octadecylsilane C_{18} (5 μm, 2.5 × 150 mm) HPLC column (Beckman, San Ramon, CA). To resolve 1-methoxy-4-nitrobenzene and the formaldehyde 2,4-dinitrophenylhydrazone, a gradient was introduced to the protocol whereby the initial concentration of 45% CH_3CN was increased to 90% (v/v). The modification of the HPLC procedure successfully resolved the peaks (see Supporting Information), although a lack of complete resolution between the peaks resulted in variability at high 1-methoxy-4-nitrobenzene concentrations.

Fitting of Steady-State Data. Initially the data were fit to both the Michaelis−Menten equation and the Hill equation. Equation 1 is the standard Michaelis−Menten equation where the velocity of the reaction is a function of the rate-limiting step in turnover (k_{cat}), the enzyme concentration ([E]), the substrate concentration ([S]), and the Michaelis constant (K_M). This equation posits a single binding site that results in the observed hyperbolic curve for turnover. Deviation from this simple scheme prompted the fit of data to the Hill equation (eq 2), which resembles the Michaelis−Menten equation except for the exponent *n*. This Hill coefficient serves as a qualitative measure of the degree of cooperativity of the system. When *n* is >1, there is positive cooperativity, whereas a value of <1 is indicative of negative cooperativity. A Hill coefficient of unity yields the Michaelis−Menten equation. Subsequently, equations were derived involving the occupation of two substrate binding sites to describe the data (see Results and Discussion). All kinetic parameters were determined using nonlinear regression with Graph-Pad Prism software (San Diego, CA). This same program was used to perform an *F* test (*28*) to determine the appropriateness of the equations as a fit of the data.

$$\frac{\nu}{[E]_t} = \frac{k_{cat}[S]}{[S] + K_M} \quad (1)$$

$$\frac{\nu}{[E]_t} = \frac{k_{cat}[S]^n}{[S]^n + K_M{}^n} \quad (2)$$

Equilibrium Binding of Ligands. P450 binding studies done to determine thermodynamic dissociation constants (K_D) typically rely on monitoring alterations of heme spectra as a function of titrant concentration. For these experiments, rabbit P450 1A2 offers very attractive absorbance properties. Nevertheless, this approach is not always feasible due to the absence of a spectral shift during binding, poor solubility of the titrant, and interference of titrant absorbance with the heme moiety. For example, the high extinction coefficient of 4-nitrophenol prevented the determination of a dissociation constant by rabbit P450 1A2 absorbance (K_S). As a complement to absorbance experiments, titrations were also performed relying on the quenching of intrinsic tryptophan fluorescence as a function of titrant concentration to provide K_F values. All titrations were performed in reaction buffer, but the concentration of enzyme used during titrations was varied depending on the respective titration method (vide infra). Regardless of the technique employed, the resulting data were fit to the typical hyperbolic curve (eq 3), where B_{max} is the amplitude of the titration and [L] is the concentration of ligand.

$$\text{signal} = \frac{B_{max}[L]}{[L] + K_D} \quad (3)$$

Alternatively, if the enzyme concentration was within 5-fold of the apparent K_D value, the data were fit to the quadratic equation (eq 4):

$$\text{signal} = A_0 + \frac{\Delta A\{(K_D + [E] + [L])^2 - 4[E][L]\}^{1/2}}{2[E]} \quad (4)$$

The initial discovery of P450s was due to spectral properties of the heme moiety. P450s exist in two states, high-spin and low-spin, the relative fractions of which reflect an intrinsic property of each P450. The spin state refers to the coordination of the heme iron. In the low-spin state, water forms a sixth ligand to iron, resulting in a λ_{max} at 420 nm. The absence of the water ligand results in a λ_{max} of 390 nm. In some cases, a binding event displaces the water molecule to shift a low-spin P450 to the high-spin state, resulting in a Type I spectrum (*14*). This is the case for rabbit P450 1A2, unlike P450 1A2 isolated from some other organisms (*18*). Another spectral shift can occur when a molecule binds and coordinates the heme iron through a nitrogen group to produce a Type II spectrum with a λ_{max} of 435 nm (*14*).

For these studies, titrations were performed using tandem cuvettes to correct for any solvent effects on P450 absorbance and possible contributions from titrant absorbance. The concentration of P450 1A2 used in titrations for 1,4-phenyldiisocyanide and 1-methoxy-4-nitrobenzene was 2.0 μM (P450 1A2 in reaction buffer), whereas titrations of 1-ethoxy-4-nitrobenzene and 1-isopropoxy-4-nitrobenzene required 0.5 μM P450 1A2 in reaction buffer due to high-affinity binding constants (low K_S values). Lower concentrations of enzyme failed to provide sufficient signal for titration experiments. The UV−visible spectra were recorded in the titration experiments using an Amino DW2a/OLIS instrument (On-Line Instrument Systems).

Fluorescence has been a very useful tool for ligand binding studies with many proteins. This is not the case for P450s due to a number of technical difficulties, which were overcome for these studies. Here, we utilized the change of intrinsic fluorescence upon binding to substrate or product. Tryptophans are excited at 295 nm to minimize tyrosine fluorescence, and the resulting fluorescence emission at 340 nm is monitored. Binding of titrant then quenches this signal. Titrations were possible for alkyl phenyl ethers although concentrations were limited due to fluorescence from the titrant itself, which is structurally similar to tyrosine. Otherwise, the fluorescence would, if possible, require correction. Specific experiments were conducted using 0.2 μM P450 1A2 in reaction buffer in a 1.0 cm path length cuvette at 25 °C. Higher enzyme concentrations caused

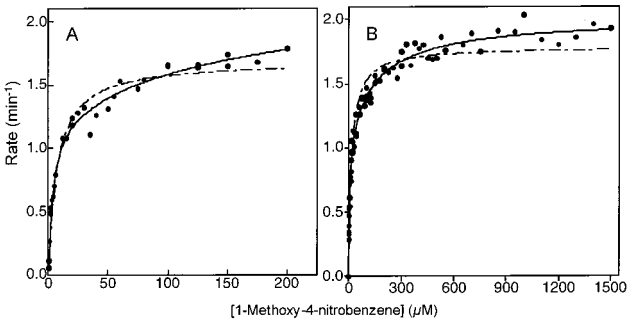

FIGURE 1: Saturation curve of rabbit P450 1A2-mediated oxidation of 1-methoxy-4-nitrobenzene following (A) 1-methoxy-4-nitrobenzene depletion and (B) 4-nitrophenol production. The data were fit to the standard Michaelis−Menten equation (dashed line) and the two binding site model (solid line). The activity was measured in a system containing purified rabbit liver P450 1A2 and rat NPR at a final concentration of 0.25 and 0.5 μM in 100 mM potassium phosphate buffer, pH 7.4, containing 50 μM DPLC at 30 °C.

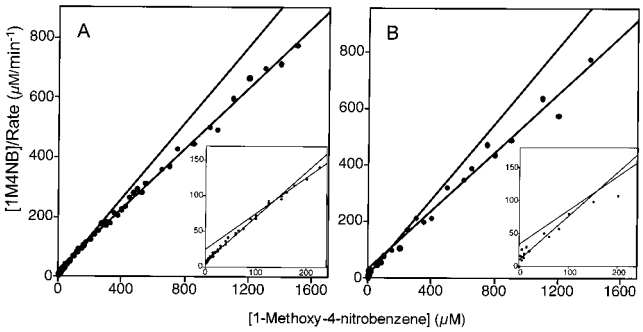

FIGURE 2: Hanes−Woolf plots ([S]/v vs [S]) of product formation rates: (A) 4-nitrophenol and (B) formaldehyde. The activity was measured in a system containing purified rabbit liver P450 1A2 and rat NPR at a final concentration of 0.25 and 0.5 μM in 100 mM potassium phosphate buffer, pH 7.4, containing 50 μM DPLC at 30 °C. The insets show expansion of portions of the data set to emphasize the nonlinearity.

excessive reflectance, which complicated the titrations. Since solutions could not be filtered, reflectance was also a problem after mixing, such that a stable signal could not be obtained until a couple minutes after the addition of titrant. The fluorescence signal was monitored using either an SPEX Fluorolog (Edison, NJ) or a Varian SF-330 spectrophotometer (Varian, Walnut Creek, CA). To determine the respective K_F values, these data were fit to the hyperbolic equation mentioned previously.

RESULTS AND DISCUSSION

The role of P450-mediated reactions in cellular processes has made the understanding of P450 mechanisms a focus of intense research. In addressing a curious but common observation in steady-state studies of P450 catalysis, we analyzed the *O*-dealkylation of 4-nitrophenyl ethers to determine the mechanism underlying the deviation from a simple Michaelis−Menten fit of the data. We pursued two strategies to shed light on our initial observation with 1-methoxy-4-nitrobenzene oxidation by rabbit P450 1A2. First, increasing the size of the *O*-alkyl group further illustrated nonhyperbolic behavior of the product formation rates as a function of substrate concentration. Second, the absorbance properties of rabbit P450 1A2 permitted an extensive set of binding studies not possible by many P450s including P450 1A2 isolated from other species (*18*). The binding competition experiments demonstrated the presence of a spectrally silent binding pool, which can only be explained by a second binding site. Taken together, we propose novel kinetic schemes for P450 1A2 to describe the steady-state data involving two substrate binding sites.

Steady-State Kinetics

Oxidation of 1-Methoxy-4-nitrobenzene. The *O*-demethylation of 1-methoxy-4-nitrobenzene was the most rigorously studied reaction in this work. Rates of 1-methoxy-4-nitrobenzene depletion could only be determined up to 200 μM due to the high intensity of the signal. These rates were plotted against substrate concentration and fit to a Michaelis−Menten scheme, where $k_{cat} = 1.69 \pm 0.03$ min^{-1} and $K_M = 7.3 \pm 0.8$ μM (Figure 1), although the data drifted from the fit at higher substrate concentrations. In contrast to substrate, the formation of the product 4-nitrophenol could be measured for substrate concentrations ranging from 0.7 to 1500 μM (Figure 1). The complete data set was fit to a simple Michaelis−Menten scheme, where $k_{cat} = 1.78 \pm 0.03$ min^{-1} and $K_M = 17.1 \pm 1.2$ μM. The large data set (total of 86 points) masked an actual poor fit of the data, as demonstrated in a Hanes−Woolf plot (Figure 2). The standard Michaelis−Menten scheme predicts a linear regression of the data; however, there is an inflection point near 150 μM substrate, which marks the intersection of lines fit to the data at low and high concentrations of substrate. Although a fit of the data to the Hill equation indicated negative cooperativity ($n < 1$), the nature of the Hill equation does not provide a mechanistic explanation for this observation and thus adds little to our understanding of P450 1A2 catalysis.

The question remains as to whether rates of formation of the product formaldehyde describe a similar trend as observed for the product 4-nitrophenol. For comparative purposes, the data are shown in a Hanes−Woolf plot (Figure 2). As observed with the 4-nitrophenol data, there is an inflection point near 150 μM substrate. High error was observed for rates obtained at substrate concentrations > 500 μM due to difficulties in resolving the peaks of 1-methoxy-4-nitrobenzene and formaldehyde 2,4-dinitrophenylhydrazone. This effect may explain why the deviation from the Michaelis−Menten scheme is less pronounced for formaldehyde production versus 4-nitrophenol production. The maximal rate of formaldehyde formation was similar to the rate of 4-nitrophenol production, 1.8 versus 2.0 min^{-1}, respectively. Taken together, the similarity of the fits between both sets of product data further discredits the possibility of spectral artifacts contributing to the signal measured at 400 nm.

A simple explanation for the deviation from the Michaelis−Menten kinetic scheme is heterogeneity of the P450 preparation, a historic problem for studies with P450s isolated from animal sources. Although no extraneous protein was visible by electrophoretic analysis, the possibility still exists that another enzyme (P450) was isolated along with the rabbit liver P450 1A2 and contributes to the steady-state rate. To eliminate this prospect, the rabbit P450 1A2 cDNA was subcloned and expressed in *E. coli*. Purified recombinant rabbit P450 1A2, devoid of other oxidases, was then assayed for activity toward 1-methoxy-4-nitrobenzene by following

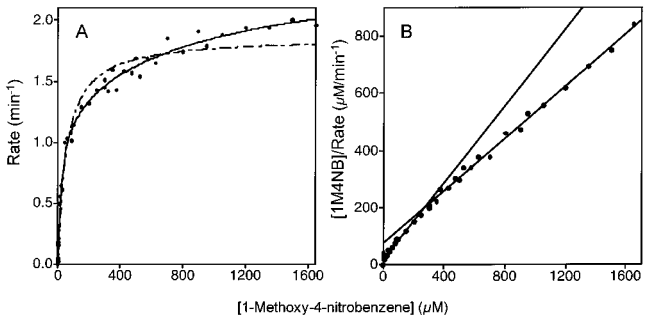

FIGURE 3: Saturation curve of recombinant rabbit P450 1A2-mediated oxidation of 1-methoxy-4-nitrobenzene following 4-nitrophenol production. (A) The data are shown in a Michaelis plot (v vs [S]) and were fit to the standard Michaelis−Menten equation (dashed line) and the two binding site model (solid line). (B) The data are also shown in a Hanes−Woolf plot ([S]/v vs [S]). The activity was measured in a system containing purified rabbit liver P450 1A2 and rat NPR at a final concentration of 0.25 and 0.5 μM in 100 mM potassium phosphate buffer, pH 7.4, containing 50 μM DPLC at 30 °C.

the formation of 4-nitrophenol (Figure 3). It is clear that this data set is significantly nonhyperbolic, which is confirmed by the Hanes−Woolf plot of the data. Compared to the results obtained with rabbit liver P450 1A2, the change in curvature reflects changes in the apparent K_M for substrate to a higher value. The alterations of the N-terminus used to improve protein expression (*18*) may contribute to the difference in apparent K_M values; however, the same maximal rate ($\sim$2 min^{-1}) was attained at higher substrate concentrations. The shift in the K_M between the two forms of rabbit P450 1A2 eliminates the possibility of substrate partitioning between micelles and the aqueous phase. Taken together, the fact that recombinant rabbit P450 1A2 demonstrates similar kinetics as liver P450 1A2 provides further evidence that the trend is not artifactual.

Multiple Oxidative Reactions. Further oxidation of the products 4-nitrophenol and formaldehyde may contribute to the complexity of the steady-state turnover of 1-methoxy-4-nitrobenzene (Scheme 1). The product 4-nitrophenol may be oxidized to 4-nitrocatechol (*29*), which would contribute to the absorbance at 400 nm (λ_{max} = 450 nm). To address this issue, the oxidation of 1-methoxy-4-nitrobenzene was followed by scanning the absorbance from 380 to 550 nm for 30 min under the same reaction conditions used in the steady-state studies. Only one peak began to appear at 400 nm, indicative of 4-nitrophenol formation (data not shown). Furthermore, 4-nitrophenol alone was not a substrate for P450 1A2. The prospect of formaldehyde oxidation by P450 1A2 is an important issue, since many studies of P450 catalysis have relied solely on monitoring the production of formaldehyde. Preliminary results from an earlier study in this lab suggested rabbit P450 1A2 could slowly oxidize formaldehyde to formic acid (unpublished results). In this study, there was no decrease in formaldehyde as determined by HPLC methods (data not shown). Although it cannot be ruled out that rabbit P450 1A2 is capable of oxidizing formaldehyde, the limit of detection in these experiments indicated the rate of formaldehyde oxidation was $<$0.1 min^{-1} at 800 μM formaldehyde, or $<$5% of the rate of formaldehyde production with saturating 1-methoxy-4-nitrobenzene. In other words, the possibility of formaldehyde oxidation by rabbit P450 1A2 is not significant. Taken together, sequential oxidations cannot account for the observed nonhyperbolic behavior.

Scheme 2: Proposed Mechanism for 1-Methoxy-4-nitrophenol Oxidation

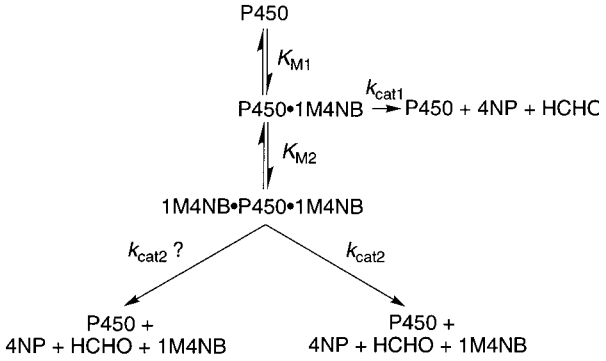

Alternative Kinetic Models To Explain Steady-State Data. From the previous experiments, it is clear that the Michaelis−Menten equation fails to appropriately describe the trend of the 1-methoxy-4-nitrobenzene data and that the observed trend is not due to artifacts from the system itself. As an alternative, we propose the two binding site mechanism shown in Scheme 2. At low concentrations of substrate, a binary complex forms and turns over to yield product; however, at higher concentrations of substrate, a ternary complex forms and introduces two possibilities depending on the orientation of the second substrate molecule. One or both substrate molecules may be poised for oxidation, which ultimately affects the apparent steady-state parameters. The program Graph-Pad Prism (San Diego, CA) was employed to fit the data to the proposed kinetic schemes. The scripts used in fitting the data are provided in the Supporting Information. Whereas the possibility of multiple substrate binding sites has been proposed for other P450s, the demonstration of this phenomenon for P450 1A2 would be novel.

In the first scenario, the binding of the second substrate molecule creates a unique Michaelis complex, which contributes more to the observed steady-state rate as the concentration of substrate increases. Equation 5 for this kinetic scheme involves two sets of parameters, k_{cat1} and K_{M1}, for the initial binary enzyme−substrate complex and k_{cat2} and K_{M2} for the ternary enzyme−substrate complex at high substrate concentrations (*30*).

$$\frac{v}{[E]_t} = \frac{k_{cat1}([S]/K_{M1}) + k_{cat2}[S]^2/K_{M1}K_{M2}}{1 + [S]/K_{M1} + [S]^2/K_{M1}K_{M2}} \qquad (5)$$

The nature of this effect on the Michaelis complex is not readily apparent. The second substrate molecule could act directly by binding to the active site or indirectly by binding to an allosteric site. This scheme has been used successfully to interpret nonhyperbolic behavior of other P450 systems (*9, 31*). Interestingly, for the oxidation of 1-methoxy-4-nitrobenzene, the k_{cat} value increased 2-fold upon binding of the second substrate molecule, suggesting the Michaelis complex is activated at higher substrate concentrations (Table 2). The higher k_{cat} value may reflect better desolvation of the active site or positioning of the substrate, although this is speculation at this point. Even though the effect is small and involves a high K_M, there have been no reports of the

Table 2: Kinetic Parameters for the Fit of the 4-Nitrophenol Data to the One-Site Kinetic Model (Equation 5)

substrate	k_{cat1} (min^{-1})	K_{M1} (μM)	k_{cat1}/K_{M1} ($min^{-1}\,\mu M^{-1}$)	k_{cat2} (min^{-1})	K_{M2} (μM)	k_{cat2}/K_{M2} ($min^{-1}\,\mu M^{-1}$)
1-methoxy-4-nitrobenzene	1.10 ± 0.08	5.2 ± 0.9	0.21 ± 0.04	2.01 ± 0.13	164 ± 26	$(12 \pm 2) \times 10^{-3}$
	$(1.2 \pm 0.1)^a$	(22 ± 3)	(0.055 ± 0.007)	(2.5 ± 0.2)	(900 ± 300)	$((2.8 \pm 0.8) \times 10^{-3})$
1-ethoxy-4-nitrobenzene	3.17 ± 0.08	3.2 ± 0.3	0.99 ± 0.09	8.7 ± 1.0	1300 ± 400	$(6.7 \pm 2.1) \times 10^{-3}$
1-isopropoxy-4-nitrobenzene	1.63 ± 0.07	1.04 ± 0.07	1.5 ± 0.1	6.0 ± 0.3	520 ± 100	$(12 \pm 2) \times 10^{-3}$

[a] Results in parentheses were obtained using recombinant rabbit P450 1A2.

Table 3: Kinetic Parameters for the Fit of the 4-Nitrophenol Data to the Two-Site Kinetic Model (Equation 6)

substrate	k_{cat1} (min^{-1})	K_{M1} (μM)	k_{cat1}/K_{M1} ($min^{-1}\,\mu M^{-1}$)	k_{cat2} (min^{-1})	K_{M2} (μM)	k_{cat2}/K_{M2} ($min^{-1}\,\mu M^{-1}$)
1-methoxy-4-nitrobenzene	1.10 ± 0.08	10.4 ± 1.8	0.11 ± 0.02	1.00 ± 0.07	82 ± 13	$(12 \pm 2) \times 10^{-3}$
	$(1.2 \pm 0.1)^a$	(43 ± 7)	(0.028 ± 0.005)	(1.2 ± 0.1)	(450 ± 150)	$((2.7 \pm 0.9) \times 10^{-3})$
1-ethoxy-4-nitrobenzene	3.17 ± 0.08	6.3 ± 0.5	0.50 ± 0.04	4.3 ± 0.5	650 ± 200	$(6.6 \pm 2.0) \times 10^{-3}$
1-isopropoxy-4-nitrobenzene	1.63 ± 0.07	2.1 ± 0.3	0.78 ± 0.11	3.0 ± 0.2	260 ± 36	$(12 \pm 2) \times 10^{-3}$

[a] Results in parentheses were obtained using recombinant rabbit P450 1A2.

alteration of P450 1A2 activity due to ligand−ligand interactions, as observed for P450 3A4 (*5*, *9*−*12*). P450 1A2 is known to activate a number of carcinogens, including aromatic and heterocyclic amines (*32*, *33*). More studies may shed light on the potential significance of this finding in the context of the metabolic role of this P450.

In the second scenario, high substrate concentrations promote the formation of a ternary Michaelis complex whereby both substrate molecules can undergo oxidation. For simplicity, it is assumed that the turnover rates of substrate in the ternary complex occur at the same rate at the respective active sites. Some proposals describing P450 3A4 catalysis include the presence of alternate unique binding sites poised for oxidation of substrate (*11*, *12*, *34*), although these investigators have not employed this particular kinetic scheme. In the absence of structural information, we can speculate that the active site of P450 1A2 can accommodate two substrate molecules in a productive complex. Equation 6 (*35*) predicts the trend of the data utilizing the same two sets of kinetic parameters as in eq 5.

$$\frac{v}{[E]_t} = \frac{2k_{cat1}([S]/K_{M1}) + 2k_{cat2}[S]^2/K_{M1}K_{M2}}{1 + 2[S]/K_{M1} + [S]^2/K_{M1}K_{M2}} \qquad (6)$$

The addition of the factor 2 accounts for the presence of the two active sites, which ultimately affects k_{cat2} and K_{M2}. The fit of the 1-methoxy-4-nitrobenzene data to this equation indicates there is no change in k_{cat} at higher substrate concentrations (Table 3). In other words, a limiting factor in substrate oxidation is the accommodation of substrate in the active site. For this mechanism, the rate of formation of the heme oxidant responsible for substrate oxidation must be greater than the observed steady-state rates. The activation of oxygen to form the heme oxidant requires the concomitant oxidation of NADPH to supply electrons via the accessory enzyme, NPR. The observation of poor coupling between NADPH utilization and 1-methoxy-4-nitrobenzene oxidation by P450 1A2 (~8% efficiency) is consistent with the possibility of a steady-state build-up of P450 poised to react with substrate (results not shown).

Oxidation of Other Alkyl 4-Nitrophenyl Ethers. If rabbit P450 1A2 can accommodate two substrate molecules, a limit can be reached due to the finite space of the active site. To address this issue in the context of our proposed kinetic models, the oxidations of 1-ethoxy-4-nitrobenzene and 1-isopropoxy-4-nitrobenzene were investigated by following the appearance of 4-nitrophenol. Consistent with the hypothesis of space limitation, the oxidation of either substrate yielded plots of 4-nitrophenol production (vs substrate concentration) that were more nonhyperbolic than the data obtained from the oxidation of 1-methoxy-4-nitrobenzene. For 1-ethoxy-4-nitrobenzene, the rates of product formation were determined for substrate concentrations from 0.5 to 1000 μM (the upper limit of substrate assayed was due to the lower solubility of this substrate). The fit of the data to the Michaelis−Menten scheme was very poor ($r^2 = 0.89$), unlike the use of either of the two binding site equations ($r^2 = 0.99$) (Figure 4). Compared to 1-methoxy-4-nitrobenzene oxidation, the turnover of 1-ethoxy-4-nitrobenzene was more efficient at low substrate concentrations, as indicated by k_{cat1}/K_{M1} (Tables 2 and 3). The larger alkyl group increased the apparent affinity for the Michaelis complex as well as increasing the rate of substrate oxidation. In contrast, at high substrate concentrations, an increased k_{cat} was offset by a much higher K_M that resulted in a 2-fold decrease in catalytic efficiency. It is likely that the larger *O*-alkyl group creates a higher affinity Michaelis complex at low substrate concentrations by possibly providing more hydrophobic contacts

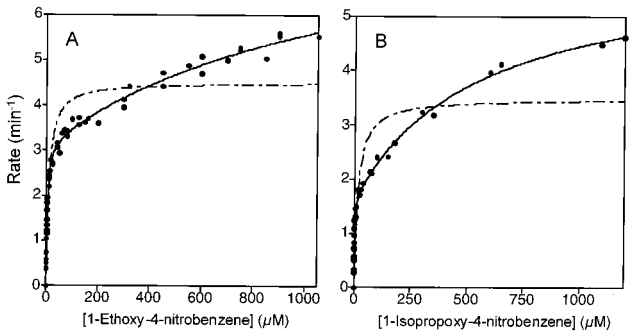

FIGURE 4: Saturation curve of rabbit P450 1A2-mediated oxidation of (A) 1-ethoxy-4-nitrobenzene and (B) 1-isopropoxy-4-nitrobenzene, using the assay for 4-nitrophenol production. The data were fit to the standard Michaelis−Menten equation (dashed line) and the two binding site model (solid line). The activity was measured in a system containing purified rabbit liver P450 1A2 and rat NPR at a final concentration of 0.25 and 0.5 μM in 100 mM potassium phosphate buffer, pH 7.4, containing 50 μM DPLC at 30 °C.

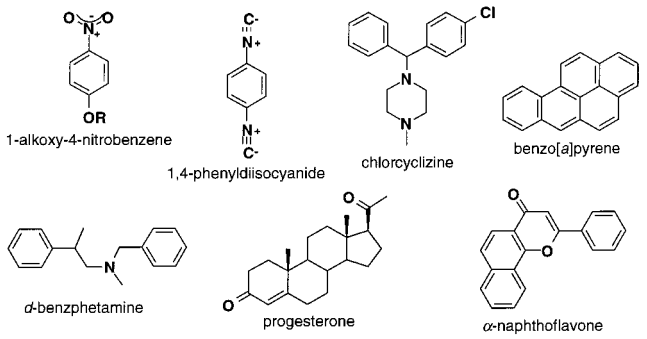

FIGURE 5: Examples of known substrates and inhibitors of rabbit P450 1A2.

and better orientation of the substrate for oxidation, but the bulkiness inhibits the formation of the second Michaelis complex.

The *O*-dealkylation of 1-isopropoxy-4-nitrobenzene demonstrated a similar trend as observed for 1-ethoxy-4-nitrobenzene. The rates of 4-nitrophenol production were determined from 0.2 to 1000 μM 1-isopropoxy-4-nitrobenzene (Figure 4), a limitation imposed by the solubility of this substrate. As observed for 1-ethoxy-4-nitrobenzene, the two substrate binding site equations provided a more acceptable fit of the data ($r^2 = 0.98$) than the standard Michaelis−Menten equation ($r^2 = 0.80$). Although the steady-state rates increased relative to 1-methoxy-4-nitrobenzene oxidation, the effect was not as significant as observed for 1-ethoxy-4-nitrobenzene turnover (Tables 2 and 3). The additional methyl group may occlude access to the α-hydrogen atom during the *O*-dealkylation reaction or increase the probability of oxidation at the methyl group. The further addition of bulkiness to the *O*-alkyl group by another methyl group enhanced the formation of the Michaelis complexes (K_{M1} and K_{M2}), but proved to decrease the maximal rate of 4-nitrophenol formation (k_{cat1} and k_{cat2}). In this case, the benefit of higher hydrophobicity to binding may result in a binding conformation whereby the substrate is not sufficiently poised for *O*-dealkylation.

The proposed mechanisms raise the following question: Is the active site of P450 1A2 large enough to accommodate two substrates? Although an ill-defined binding site is characteristic of P450s, there have been no reports to date that demonstrate the existence of more than one binding site on P450 1A2. Based on the X-ray crystal structure of bacterial P450 102, Lozano et al. (*36*) reported a homology model of the human P450 1A2 enzyme that predicted a wide but thin hydrophobic active site. A survey of typical P450 1A2 substrates reveals a preference for small, planar molecules with some notable exceptions (*32*, *37*). Rabbit P450 1A2 does bind large molecules including chlorcyclizine (*38*), α-naphthoflavone, benzo[*a*]pyrene (*39*), *d*-benzphetamine (*38*, *40*), and progesterone (*41*) (Figure 5). In light of these reports, it is conceivable that the binding space occupied by these large molecules could accommodate two smaller alkyl 4-nitrophenyl ethers. Nonetheless, in the absence of further studies, it is not possible to distinguish between these mechanisms.

Equilibrium Binding of Ligands

A key to the argument for multiple binding sites is the actual observation of the binding of one or more molecules to the enzyme. We employed two techniques to obtain equilibrium dissociation binding constants (K_D) based on either absorbance (K_S) or fluorescence (K_F) signals. These two options provided a means of overcoming technical difficulties that obviated the use of one of the techniques. An attractive quality of rabbit P450 1A2 is the low-spin character of the free enzyme (*18*). Since 4-nitrophenol masked the P450 absorbance signal, the quench of intrinsic tryptophan fluorescence was used to obtain binding data. As a confirmation of the complementarity of these techniques, the titration of phenacetin by the absorbance or fluorescence techniques yielded K_D values within error of each other, $K_S = 13 \pm 1$ μM and $K_F = 12 \pm 1$ μM, respectively, as in the case of human P450 1A2 (*42*). All data sets fit well to the standard hyperbolic curve, suggesting the signals reflect a single binding event.

The complement of these spectroscopic techniques enabled the determination of K_D values for both substrates and product 4-nitrophenol. Where appropriate, titrations were performed using titrant concentrations up to 100 times the K_S determined by a fit to the standard hyperbolic equation to ensure saturation of the binding site(s). The binding of the alkyl 4-nitrophenyl ethers by rabbit P450 1A2 demonstrated typical Type I spectra (data not shown). The size of the *O*-alkyl group greatly affected the affinity of the alkyl 4-nitrobenzenes for rabbit P450 1A2, as judged by the results of these absorbance titrations. The binding affinity of 1-methoxy-4-nitrobenzene was weak ($K_S = 112 \pm 11$ μM), whereas the bulkier 1-isopropoxy-4-nitrobenzene displayed an almost 200-fold higher affinity for rabbit P450 1A2 ($K_S = 0.59 \pm 0.05$ μM) and the K_S value for 1-ethoxy-4-nitrobenzene was intermediate between these values ($K_S = 3.6 \pm 0.1$ μM). These large changes in affinity reflect the sensitivity of the active site to minor structural differences between the alkyl 4-nitrophenyl ethers. The interaction between P450 1A2 and NPR did not affect the affinity of P450 1A2 for substrate, since the K_S value for 1-methoxy-4-nitrophenol by this complex was 96 ± 15 μM as determined by an absorbance titration (0.2 μM P450 1A2, 0.4 μM rat NPR). The strong absorbance signal of product 4-nitrophenol obviated the use of heme absorbance to obtain a K_D value. In this case, the fluorescence technique provided a suitable signal to determine the dissociation constant for 4-nitrophenol ($K_F = 55 \pm 5$ μM). The addition of formaldehyde (to 1000 μM) did not affect either the absorbance or the fluorescence of rabbit P450 1A2. Presumably the affinity is very low for formaldehyde, although a K_D value could not be determined.

Binding Competition between Two Titrants. On the basis of the analysis of the steady-state data, the possibility was considered that the binding site of rabbit P450 1A2 accommodates two substrate molecules. The previous titrations of individual compounds did not reveal unusual binding events, or at least the data fit well to a hyperbolic function. An indirect way to assess the possibility of two binding sites for rabbit P450 1A2 is to perform binding competition studies. How two titrants compete for binding to the enzyme is indicative of the availability of site(s) on the enzyme. Here, our strategy was to utilize two titrants that provide different spectroscopic signals upon formation of the bound complex. To this end, we relied on the different types of heme absorbance spectra resulting from the binding event. The

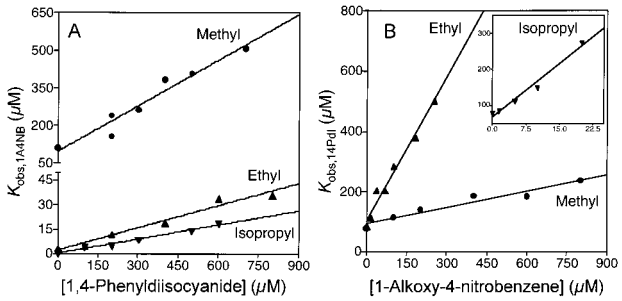

FIGURE 6: Competitive binding studies. For both panels, the symbols (●), (▲), and (▼) represent data obtained for 1-methoxy-4-nitrobenzene, 1-ethoxy-4-nitrobenzene, and 1-isopropoxy-4-nitrobenzene, respectively. (A) Plot of observed dissociation constants for alkyl 4-nitrophenyl ethers (1A4NB) as a function of 1,4-phenyldiisocyanide concentration. (B) Plot of observed dissociation constants for 1,4-phenyldiisocyanide as a function of concentration of alkyl 4-nitrophenyl ethers.

Table 4: Effect of Competing Ligand on the Apparent K_S for 1,4-Phenyldiisocyanide

competing ligand	K_S (μM) for 1,4-phenyldiisocyanide
none	78 ± 6
1-methoxy-4-nitrobenzene	190 ± 20
1-ethoxy-4-nitrobenzene	80 ± 7
1-isopropoxy-4-nitrobenzene	20 ± 2

interaction of the alkyl 4-nitrophenyl ethers with rabbit P450 1A2 resulted in typical Type I spectra, whereas the binding of 1,4-phenyldiisocyanide was found to provide a Type II spectrum. 1,4-Phenyldiisocyanide shares structural similarity to the 4-nitrophenyl ethers of this study (Figure 5). Binding titrations of one ligand in the presence of the other ligand produced either a shift from a Type I to a Type II spectrum or vice versa. Two different approaches were used to interpret the resulting data, a single binding site model and a two binding site model.

One Binding Site Model. If only one site exists on the enzyme, then the competition between two ligands for that site follows a predictable relationship described by eq 7 (*43*).

$$K_{A,obs} = [B](K_A/K_B) + K_A \quad (7)$$

The titration of ligand A in the presence of ligand B produces an observed dissociation constant ($K_{A,obs}$) which varies linearly with the concentration of ligand B. If only one site exists for these compounds, the apparent dissociation constant for ligand B (K_B) derived from the competition experiments is equal to the value measured in the absence of the competing ligand A.

As predicted, the competitive binding studies yielded linear relationships between the titrants. A plot of the $K_{S,obs}$ values for the alkyl 4-nitrophenyl ethers in the presence of 100−800 μM 1,4-phenyldiisocyanide is shown in Figure 6. For all alkyl 4-nitrophenyl ethers, the data were fit to a linear regression described by eq 7. Surprisingly, the size of the *O*-alkyl group greatly affected the apparent K_S value for 1,4-phenyldiisocyanide, as summarized in Table 4. In the absence of competing titrant, 1,4-phenyldiisocyanide bound with a K_S of 78 ± 6 μM. This value increased 2.5-fold upon addition of the isosteric compound 1-methoxy-4-nitrobenzene but decreased 4-fold in titrations with 1-isopropoxy-4-nitrobenzene. The apparent K_S for 1,4-phenyldiisocyanide was unchanged in the presence of 1-ethoxy-4-nitrobenzene.

Scheme 3: Ordered Binding of Ligand for the Two Binding Site Model

$$\text{P450} \overset{K_A}{\rightleftharpoons} \text{P450•A} \overset{K_{AA}}{\rightleftharpoons} \text{A•P450•A}$$

Table 5: Effect of 1,4-Phenyldiisocyanide on the Apparent K_S for Alkyl 4-Nitrophenyl Ethers

titrant	K_S (μM)[a] − 14PdI	K_S (μM)[b] + 14PdI
1-methoxy-4-nitrobenzene	112 ± 11	430 ± 60
1-ethoxy-4-nitrobenzene	3.6 ± 0.1	47 ± 2
1-isopropoxy-4-nitrobenzene	0.59 ± 0.05	7.9 ± 0.6

[a] Values in the absence of 1,4-phenyldiisocyanide (14PdI). [b] Values in the presence of 1,4-phenyldiisocyanide (14PdI).

In the reverse experiment, the plot of the $K_{S,obs}$ values for the 1,4-phenyldiisocyanide in the presence of varying concentrations of the respective alkyl 4-nitrophenyl ether is shown in Figure 6. Due to the variation in affinity for the alkyl 4-nitrophenyl ethers, each competitive binding study involved different ranges of competing titrant. The concentrations of 1-methoxy-4-nitrobenzene, 1-ethoxy-4-nitrobenzene, and 1-isopropoxy-4-nitrobenzene used in the study were in the range of 100−800 μM, 15−250 μM, and 1.5−20 μM, respectively. All three data sets were fit to a linear regression to yield the apparent K_S values for the alkyl 4-nitrophenyl ethers in the presence of 1,4-phenyldiisocyanide (Table 5). As observed for 1,4-phenyldiisocyanide, there were differences between the equilibrium dissociation constants obtained for the alkyl 4-nitrophenyl ethers and the values derived from the competitive binding experiments. The competition between the ligands raised the K_S values 4-fold for 1-methoxy-4-nitrobenzene and 13-fold for both 1-ethoxy-4-nitrobenzene and 1-isopropoxy-4-nitrobenzene. Taken together, the obvious dependence of the K_S values on the presence of a competing titrant invalidates the single binding site model.

Two Binding Site Model. As an alternative, we constructed a binding mechanism consistent with Scheme 2 for substrate turnover, namely, the inclusion of binary and ternary enzyme−substrate complexes. The program DYNAFIT (*44*) was used to estimate dissociation constants for titrants in the absence or presence of competing titrant. A fit of the data to a two binding site mechanism required a minimizing of the variables since both the respective dissociation constants and the spectral amplitudes of the liganded complexes are unknown. The DYNAFIT scripts used in the fitting of the data are in the Supporting Information. It was assumed that the affinity of ligand for the second site was weak, such that binding is effectively an ordered process. The interaction between the enzyme and titrant is described in Scheme 3, where K_A is the dissociation constant for the binary complex and K_{AA} is the dissociation constant for the ternary complex. The variables for the fit included the K_S parameters as well as the spectral amplitudes for the respective liganded complexes.

The fit of these data to Scheme 4 yielded both a high-affinity component (K_A or K_B) and a low-affinity component (K_{AA} or K_{BB}). As observed earlier from the fit of the data to the standard hyperbolic equation, the affinity of rabbit P450 1A2 was similar for 1,4-phenyldiisocyanide and 1-methoxy-4-nitrobenzene. In this case, the high-affinity component was

Scheme 4: Ligand Competition for the Two Binding Sites

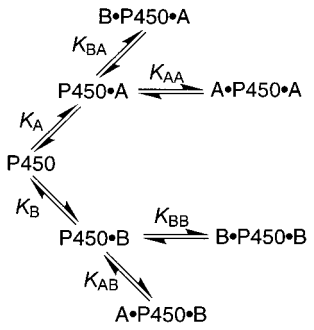

Table 6: Equilibrium Dissociation Constants for the Two Binding Site Model (Schemes 4 and 5)

titrant[a]	K_S (μM)[b]	spectral amplitude
1,4-phenyldiisocyanide		
K_A (P450·14PdI)	19 ± 4[c]	0.0087 ± 0.0007
K_{AA} (14PdI·P450·14PdI)	280 ± 60[c]	0.0285 ± 0.0007
K_{BA} (1M4NB·P450·14PdI)	102 ± 3[d]	0.0559 ± 0.0007
K_{AB} (14PdI·P450·1M4NB)	244 ± 20[d]	*e*
1-methoxy-4-nitrobenzene		
K_B (P450·1M4NB)	16 ± 4[c]	0.0037 ± 0.0003
K_{BB} (1M4NB·P450·1M4NB)	270 ± 90[c]	0.0149 ± 0.0004
K_{AB} (14PdI·P450·1M4NB)	240 ± 11[d]	0.0213 ± 0.0004
K_{BA} (1M4NB·P450·14PdI)	157 ± 12[d]	*e*

[a] The titrants 1,4-phenyldiisocyanide and 1-methoxy-4-nitrobenzene are indicated by 14PdI and 1M4NB, respectively. [b] Dissociation constants reflect values for the underlined titrant. [c] Values determined fitting binding data to Scheme 4. [d] Values determined fitting binding data to Scheme 5. [e] The fit of the data to Scheme 5 included the assumption that the spectral binding event involves only one binding site.

$\sim$17 μM, and the low-affinity component was $\sim$275 μM (Table 6). The magnitude of the difference between the dissociation constants for 1-methoxy-4-nitrobenzene is similar to the difference between the apparent K_M values derived from the kinetic models (Tables 2 and 3). The significance of this observation is unknown in the absence of further study. A common explanation is that there exists a rate-limiting step following chemistry, for evidence exists in the case of P450 2E1 catalysis (*45*). Unfortunately, for 1-ethoxy-4-nitrobenzene and 1-propoxy-4-nitrobenzene, attempts to fit the data to Scheme 4 resulted in a high-affinity component well below the enzyme concentration and therefore could not be determined with sufficient accuracy.

The addition of a second titrant introduces the possibility of not only homogeneous complexes for the ligands but also heterogeneous complexes as well (Scheme 4). The binding data from 1,4-phenyldiisocyanide and 1-methoxy-4-nitrobenzene studies were fit globally to the proposed two binding site model. These two data sets offer an internal test for the proposed model, since the fit of each data set will produce the dissociation constants for the same heterogeneous liganded complexes. If the model is correct, the same values should be obtained by each data set. The variables for the fit included the dissociation constants for the mixed ligand complexes and the spectral amplitudes of all possible liganded complexes. As shown in Table 6, the agreement between the dissociation constants for the heterogeneous complexes indicates that the two binding site model is a suitable solution for the data obtained through competitive binding studies. Interestingly, the identity of the molecule in the high-affinity site produced different effects on the affinity of the titrants for the second binding site. For 1,4-phenyldiisocyanide, the affinity for the second site increased approximately 2.5-fold in the presence of 1-methoxy-4-nitrobenzene relative to the occupancy of 1,4-phenyldiisocyanide in the low-affinity site. In contrast, the affinity of 1-methoxy-4-nitrobenzene for the second site did not depend on the occupancy of either compound in the high-affinity site.

Concluding Remarks. Although most P450 reactions demonstrate saturation kinetics that can be fit to the standard Michaelis−Menten equation, there are numerous exceptions where sigmoidal or nonhyperbolic behavior is observed. Several groups have employed kinetic models involving two binding sites that appropriately described the trend observed in the data. Unlike those studies, we demonstrated the consistency of a two binding site model to interpret both steady-state kinetics and binding events. The complement of these two data sets, as well as the elimination of potential artifacts, provides more credence for the application of the two binding site model. This novel finding for P450 1A2 may be more common than originally perceived, as reports citing atypical kinetics for a variety of P450s continue to increase (*9*−*12*, *31*). Only through a more rigorous analysis of potential models of P450 catalysis are we to realize the ultimate goal of predicting P450 catalytic properties for applications as diverse as drug design, bioremediation, and cancer risk estimation may be realized.

ACKNOWLEDGMENT

We acknowledge Drs. H. Cai for acquiring NMR and mass spectra and M. V. Martin for purification of rabbit liver P450 1A2.

SUPPORTING INFORMATION AVAILABLE

Figure showing HPLC separation of formaldehyde 2,4-dinitrophenylhydrazone and DYNAFIT scripts used for estimating binding constants for two binding site models (Schemes 3 and 4) (5 pages). This material is available free of charge via the Internet at http://pubs.acs.org.

REFERENCES

1. Palmer, G., and Reedijk, J. (1992) *J. Biol. Chem. 267*, 665−677.
2. Coon, M. J., Ding, X., Pernecky, S. J., and Vaz, A. D. N. (1992) *FASEB J. 6*, 669−673.
3. Ortiz de Montellano, P. R., Ed. (1995) in *Cytochrome P450: Structure, Mechanism, and Biochemistry*, Plenum Press, New York.
4. Testa, B. (1995) in *Biochemistry of Redox Reactions*, Academic Press, London.
5. Ueng, Y.-F., Kuwabara, T., Chun, Y.-J., and Guengerich, F. P. (1997) *Biochemistry 36*, 370−381.
6. Schwab, G. E., Raucy, J. L., and Johnson, E. F. (1988) *Mol. Pharmacol. 33*, 493−499.
7. Johnson, E. F., Schwab, G. E., and Vickery, L. E. (1988) *J. Biol. Chem. 263*, 17672−17677.
8. Kerr, B. M., Thummel, K. E., Wurden, C. J., Klein, S. M., Kroetz, D. L., Gonzalez, F. J., and Levy, R. H. (1994) *Biochem. Pharmacol. 47*, 1969−1979.
9. Korzekwa, K. R., Krishnamachary, N., Shou, M., Ogai, A., Parise, R. A., Rettie, A. E., Gonzalez, F. J., and Tracy, T. S. (1998) *Biochemistry 37*, 4137−4147.

10. Shou, M., Mei, Q., Ettore, M. W., Jr., Dai, R., Baillie, T. A., and Rushmore, T. H. (1999) *Biochem. J. 340*, 845−853.
11. Hosea, N. A., Miller, G. P., and Guengerich, F. P. (2000) *Biochemistry 39*, 5929−5939.
12. Houston, J. B., and Kenworthy, K. E. (2000) *Drug Metab. Dispos. 28*, 246−254.
13. Shou, M., Dai, R., Cui, D., Korzekwa, K. R., Baillie, T. A., and Rushmore, T. H. (2001) *J. Biol. Chem. 276*, 2256−2262.
14. Schenkman, J. B., Remmer, H., and Estabrook, R. W. (1967) *Mol. Pharmacol. 3*, 113−123.
15. Alker, D., Campbell, S. F., and Cross, P. E. (1991) *J. Med. Chem. 34*, 19−24.
16. Bamkole, T. O., Hirst, J., and Udoessien, E. I. (1973) *J. Chem. Soc., Perkin Trans. 2 15*, 2114−2119.
17. Alterman, M. A., and Dowgii, A. I. (1990) *Biomed. Chromatogr. 4*, 221−222.
18. Sandhu, P., Guo, Z., Baba, T., Martin, M. V., Tukey, R. H., and Guengerich, F. P. (1994) *Arch. Biochem. Biophys. 309*, 168−177.
19. Omura, T., and Sato, R. (1964) *J. Biol. Chem. 239*, 2370−2378.
20. Guengerich, F. P. (2001) *Principles and Methods of Toxicology* (Hayes, A. W., Ed.) pp 1625−1687, Taylor & Francis, New York.
21. Yun, C.-H., Ahn, T., and Guengerich, F. P. (1998) *Arch. Biochem. Biophys. 356*, 229−238.
22. Shen, A. L., Porter, T. D., Wilson, T. E., and Kasper, C. B. (1989) *J. Biol. Chem. 264*, 7584−7589.
23. Hanna, I. H., Teiber, J. F., Kokones, K. L., and Hollenberg, P. F. (1998) *Arch. Biochem. Biophys. 350*, 324−332.
24. Nash, T. (1953) *Biochem. J. 55*, 416−421.
25. Quesenberry, M. S., and Lee, Y. C. (1996) *Anal. Biochem. 234*, 50−55.
26. Yoo, J. S. H., Guengerich, F. P., and Yang, C. S. (1988) *Cancer Res. 48*, 1499−1504.
27. Shu, L., and Hollenberg, P. F. (1996) *Carcinogenesis 17*, 569−576.
28. Yamaoka, K., Nakagawa, T., and Uno, T. (1978) *J. Pharmacokinet. Biopharm. 6*, 165−175.
29. Koop, D. R. (1992) *FASEB J. 6*, 724−730.
30. Segel, I. H. (1975) *Enzyme Kinetics: Behavior and Analysis of Rapid Equilibrium and Steady-state Enzyme Systems*, pp 355−356, John Wiley & Sons, New York.
31. Inouye, K., Mizokawa, T., Saito, A., Tonomura, B., and Ohkawa, H. (2000) *Biochim. Biophys. Acta 1481*, 265−272.
32. Kadlubar, F. F., and Hammons, G. J. (1987) in *Mammalian Cytochromes P-450* (Guengerich, F. P., Ed.) Vol. 2, pp 81−130, CRC Press, Boca Raton, FL.
33. Butler, M. A., Iwasaki, M., Guengerich, F. P., and Kadlubar, F. F. (1989) *Proc. Natl. Acad. Sci. U.S.A. 86*, 7696−7700.
34. Harlow, G. R., and Halpert, J. R. (1998) *Proc. Natl. Acad. Sci. U.S.A. 95*, 6636−6641.
35. Segel, I. H. (1975) *Enzyme Kinetics: Behavior and Analysis of Rapid Equilibrium and Steady-state Enzyme Systems*, pp 382−384, John Wiley & Sons, New York.
36. Lozano, J. J., López-de-Briñas, E., Centeno, N. B., Sanz, F., and Guigo, R. (1997) *J. Comput.-Aided Mol. Des. 11*, 395−408.
37. Landi, M. T., Sinha, R., Lang, N. P., and Kadlubar, F. F. (1999) in *Metabolic Polymorphisms and Susceptibility to Cancer* (Ryder, W., Ed.) pp 173−193, IARC Scientific Publications, Lyon.
38. Koop, D. R., and Coon, M. J. (1979) *Biochem. Biophys. Res. Commun. 91*, 1075−1081.
39. Schrader, W., and Linscheid, M. (1997) *Arch. Toxicol. 71*, 588−595.
40. Chiang, J. Y. L. (1981) *Arch. Biochem. Biophys. 211*, 662−673.
41. Lange, R., Balny, C., and Maurel, P. (1984) *Biochem. Pharmacol. 33*, 2771−2776.
42. Yun, C.-H., Miller, G. P., and Guengerich, F. P. (2000) *Biochemistry 39*, 11319−11329.
43. Segel, I. H. (1975) in *Enzyme Kinetics: Behavior and Analysis of Rapid Equilibrium and Steady-state Enzyme Systems*, p 109, John Wiley & Sons, New York.
44. Kuzmic, P. (1996) *Anal. Biochem. 237*, 260−273.
45. Bell-Parikh, L. C., and Guengerich, F. P. (1999) *J. Biol. Chem. 274*, 23833−23840.

BI010402Z